Journal of Materials Chemistry

www.rsc.org/materials

Volume 19 | Number 10 | 14 March 2009 | Pages 1341–1504

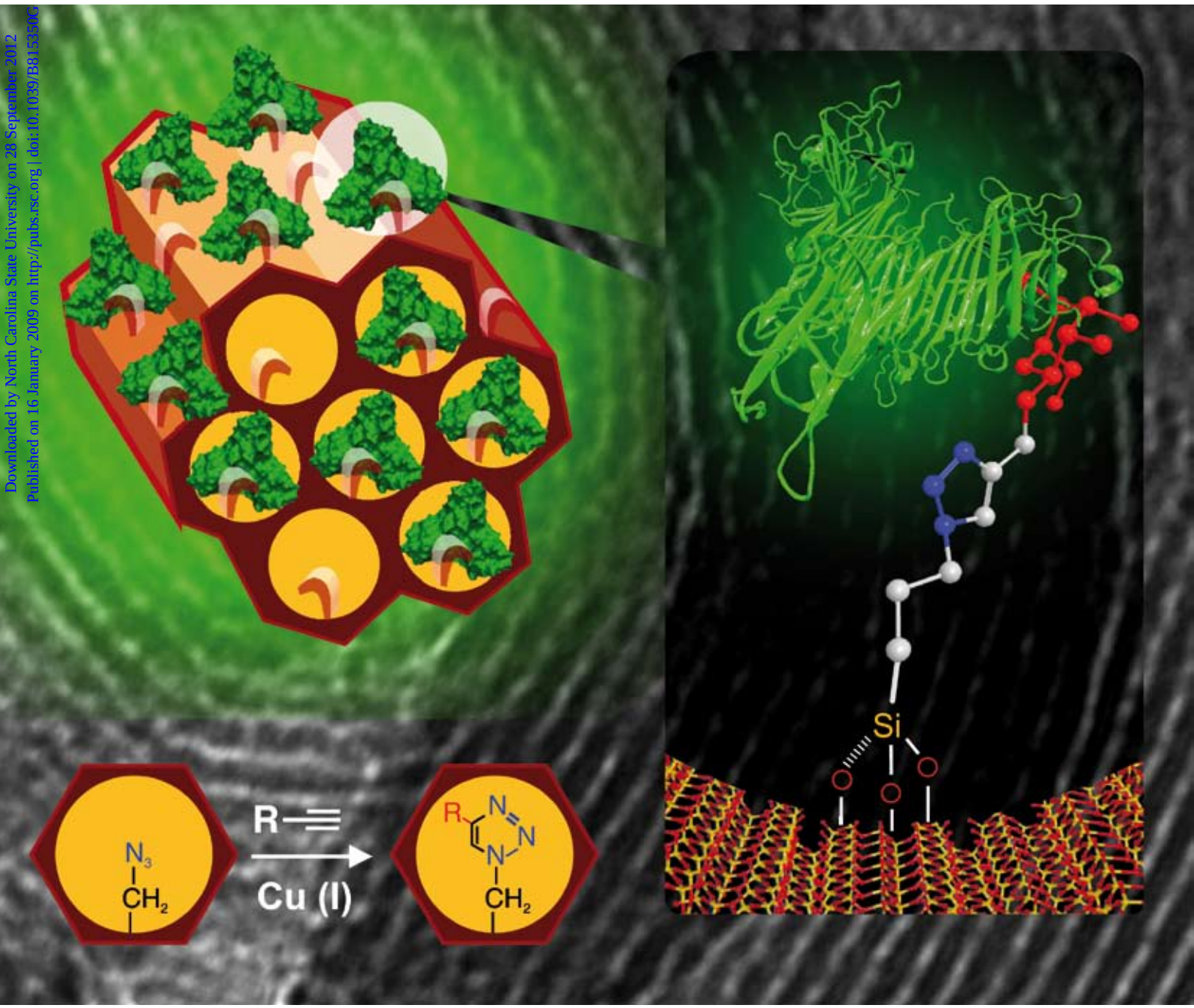

ISSN 0959-9428

RSC Publishing

"Clickable" SBA-15 mesoporous materials: synthesis, characterization and their reaction with alkynes†

Bharmana Malvi,[a] Bibhas R. Sarkar,[a] Debasis Pati,[a] Renny Mathew,[b] T. G. Ajithkumar[b] and Sayam Sen Gupta*[a]

Received 3rd September 2008, Accepted 24th November 2008
First published as an Advance Article on the web 16th January 2009
DOI: 10.1039/b815350g

SBA-15 mesoporous silica has been functionalized with azidopropyl groups through both one-pot co-condensation and post-synthetic grafting. For both these methodologies, azidopropyltriethoxysilane was used to introduce the azidopropyl groups. The azidopropyl modified SBA-15 material synthesized by one-pot co-condensation had hexagonal crystallographic order, pore diameters up of 50 Å, and the content of azidopropyl groups was found to be 1.3 mmol g^{-1}. The presence of the azidopropyl group was confirmed by multinuclear (^{13}C, ^{29}Si) solid state NMR and IR spectroscopy. Both these materials underwent very efficient Cu(I)-catalyzed azide alkyne "click" reaction (CuAAC) with a variety of alkynes. Nearly 85% of the azide present in the SBA-15 material was converted to the corresponding triazole when propargyl alcohol was used as the substrate. This methodology was also used to incorporate mannose into SBA-15. Incubation of this mannose labeled SBA-15 with fluorescein labeled Concanavalin-A led to the formation of a fluorescent silica-protein hybrid material. The ease of synthesis for the azide labeled SBA-15 material together with its ability to undergo very efficient chemoselective CuAAC in water would make it a very attractive platform for the development of covalently anchored catalysts, enzymes and sensors.

Introduction

Surface functionalized mesoporous materials have emerged as one of the most important research areas in the field of advanced functional materials.[1–3] They have found wide spread applications in catalysis,[4–6] separation,[7,8] decontamination,[9] drug delivery[10] and sensor design.[11] In particular, mesoporous siliceous matrices like SBA-15 are ideal candidates for functionalization due to their high hydrothermal stability, large pore sizes (~90–100Å) and thick walls that can be easily functionalized using simple silanol chemistry.[12,13] SBA-15 has been functionalized with various organic functional groups. These include amines,[14,15] thiols,[16] carboxylic acid,[17] sulfonic acid,[18] vinyl[19] and nitrogen based heterocycles.[9] In general, formulation of a siliceous SBA-15 with covalently linked functional groups can be designed using two different synthetic strategies for surface modification. These are post-synthesis modification (also known as grafting), and direct synthesis or co-condensation.[20] Grafting involves covalent attachment of organic functional groups to the surface of the mesoporous material by the reaction of a suitable functional group bearing organosilane. In contrast, direct synthesis or co-condensation involves modification of the surface in a single step, by co-condensation of organosilane with the silica precursor in the presence of a liquid crystalline template. Both methods have their respective advantages and drawbacks. The most significant advantage of the co-condensation method over the grafting method is the uniform distribution of organic groups on the surface of SBA-15, and higher loading of organic functionalities without reducing the pore size of SBA-15. The functional groups installed by such modifications can be used to anchor various synthetic catalysts, biomolecules and polymers to generate novel functional materials.

Development of mesoporous material based biocatalysts[21–24] and biosensors[11] has attracted a lot of attention currently. Most of these materials have been prepared by immobilization of the enzymes into the pores of the mesoporous channels by physical adsorption.[25,26] Although simple and efficient, this process is severely limited by the fact that with time, the proteins or enzymes leach out into the solution. To overcome this, enzymes have been covalently immobilized by chemically attaching them to an organo-functionalized mesoporous material bearing aldehyde or amine functional groups. Most of the effort has been directed towards cross linking the amine side-chain of the lysine to the aminopropyl group of modified mesoporous materials *via* glutaraldehyde.[27–29] For example, Wang *et al.* have covalently immobilized trypsin to a propanal modified SBA-15 *via* the imine forming reaction.[29] Both these methods have severe limitations, primarily due to limited control of the spatial orientation of the immobilized enzyme within the pores. For example, the orientation of the immobilized enzyme may be such that the active site faces the wall of the mesopore. This would make the enzyme ineffective and indeed be an obstacle in the development of such materials. Hence, there is a need to generate functional

[a]*CReST, Chemical Engineering Division, National Chemical Laboratory, Dr. Homi Bhabha Road, Pune, 411008, India*
[b]*Central NMR Facility, National Chemical Laboratory, Dr. Homi Bhabha Road, Pune, 411008, India. E-mail: ss.sengupta@ncl.res.in; Fax: +91 20 25902621; Tel: +91 20 25902747*

† Electronic supplementary information (ESI) available: Further synthesis details; BET surface area and pore size analysis; calibration curve for semi-quantitative determination of azide groups in SBA-15; ^{29}Si MAS spectra of the different functionalized SBA-15 materials. See DOI: 10.1039/b815350g

mesoporous materials which can provide a platform to perform bioorthogonal chemoselective ligation.[30] This would provide spatial control over the molecule, such that it may be attached to the silica support at the desired orientation.

The recent discovery of the Cu(I)-catalyzed 1,3-dipolar cycloaddition of organic azides to alkynes has provided the most powerful "click chemistry" tool for conjugation between appropriately functionalized binding partners *via* a 1,2,3-triazole linkage.[31] The favorable thermodynamics, exceptionally high yields, ease and compatibility with a broad repertoire of functional groups has led to numerous applications of Cu(I)-catalyzed azide-alkyne click chemistry (CuAAC) reaction in various fields of organic, medicinal, polymer, materials and biological chemistry.[32–34] CuAAC has been successfully used to functionalize metal nanoparticles,[35] single-walled carbon nanotubes,[35] powdered silica,[36,37] and mesoporous silicon rugate filters.[38] Importantly, one of the most promising applications of this reaction has been in bioconjugation reactions where it has been shown to be much more effective than traditional methods.[39] Therefore, synthesis of azide containing SBA-15 materials would be very useful in the development of functional materials. The presence of an organic azide on SBA-15 gives a handle to anchor various moieties such as enzymes and catalysts *via* this chemoselective ligation.

This study reports the synthesis and characterization of an SBA-15 mesoporous material containing a clickable azide group, and demonstrates its reactions with a number of functional organic molecules bearing alkyne functionality using CuAAC. These materials were characterized by using FT-IR, powder XRD, SEM, TEM, multinuclear (^{13}C, ^{29}Si) solid state NMR, and BET analysis. Further, this study discusses the binding of fluorescein-labeled protein Concanavalin-A to SBA-15 conjugated with mannose.

Experimental

Synthesis

Synthesis of 3-azidopropyltriethoxysilane, AzPTES. 3-Chloropropyltriethoxysilane (abbreviated as Cl-PTES; 2 g, 8.3 mmol) was added to a solution of sodium azide (1.08 g, 16.6 mmol) and tetrabutylammonium bromide (0.644 g, 2 mmol) in dry acetonitrile (50 mL), under nitrogen atmosphere. The reaction mixture was stirred under reflux for 18 h. After completion of the reaction, the solvent was removed under reduced pressure. The crude mixture was diluted in n-pentane and the suspension was filtered over Celite. Solvent was removed from the resulting filtrate and the crude oil obtained was distilled under reduced pressure of 0.025 mbar at 62 °C to give AzPTES (3-azidopropyltriethoxysilane) as a colorless liquid. Yield: 1.52 g, 74%. ^1H NMR (500 MHz, $CDCl_3$): δ 0.66 (t, 2H, J = 8.25 Hz), 1.21 (t, 3H, J = 6.88 Hz), 1.66–1.73 (m, 2H), 3.25 (t, 2H, J = 7.16 Hz), 3.80 (q, 2H, J = 6.88 Hz). ^{13}C NMR (50 MHz, $CDCl_3$) δ 7.59, 18.23, 22.64, 53.8, 58.41. FT-IR (NaCl, cm^{-1}): 2098 (-N=N^+=N^-, s).

Synthesis of SBA-15. SBA-15 material was synthesized following the procedure reported by Zhao *et al.*,[12] with slight modifications. In a typical batch synthesis, 8 g of the nonionic block copolymer Pluronic P123 was taken in a polypropylene beaker and 60 mL distilled deionized water was added to it. The mixture was stirred thoroughly using an overhead stirrer (with teflon blades) for 4 h to dissolve the gel completely. To this solution, 240 mL of HCl (2 N) were added dropwise, and the reaction mixture was allowed to stir for another 1 h at ambient temperature (~301–303 K). The temperature of the mixture was then raised to 313 K and it was allowed to proceed for another hour. To this warm mixture, tetraethylorthosilicate (TEOS, 18 g, 86.4 mmol) was added dropwise with vigorous stirring. Upon the completion of addition, the mixture was allowed to stir for 24 h while maintaining the temperature at 313 K. The synthesis gel thus formed was then loaded in a 500 mL polypropylene bottle, sealed using teflon tape and kept at 373 K for 48 h under static conditions. After this, the bottle was removed from the oven, and was allowed to cool to ambient temperature. The contents were then filtered and the residue was washed with copious amount of water until the pH of the water became neutral. The white solid was allowed to dry in air, and then crushed using a mortar and pestle. Calcination of the as-synthesized solid material was done at 773 K for 6 h in air, using a slow heating ramp of 1 degree per minute. The sample was cooled to ambient temperature and preserved under argon atmosphere for further use. Yield: ~ 4.7 g. This material will be represented as CAL-SBA-15.

Synthesis of azide functionalized SBA-15 (one-pot co-condensation technique). For the functionalization of SBA-15 using the one-pot co-condensation technique, the typical synthesis of SBA-15 as described previously was modified following the strategies described by Wang *et al.*[15] The composition of the synthesis gel was 0.9 TEOS : 0.1 AzPTES : 6.1 HCl : 0.017 P123 : 165 H_2O. In a typical synthesis batch, 4 g of Pluronic P123 was dissolved in 30 mL H_2O for 4 h, to this 120 mL of 2N HCl was added and stirred for another 1 h at ambient temperature. The temperature was raised to 313 K and the mixture was stirred at 313 K for a further 1 h. Then 8.1 g TEOS were added dropwise and the mixture was allowed to prehydrolyze for 3 h before the addition of 1.1 g of AzPTES, after which it was allowed to stir for a total of 24h (including prehydrolysis) at 313 K. The mixture was transferred to a 250 mL polypropylene vessel and heated at 373 K for 48 h under static conditions. The contents were cooled, filtered, washed with water and dried. The white solid was then refluxed in ethanol for 24 h (200 mL ethanol per 1.5 g of solid), filtered and dried to get the azide-functionalized SBA-15. Yield: ~2.9 g. This material will be referred as AZP-SBA-C.

Synthesis of azide functionalized SBA-15 (post-synthesis grafting technique). To a suspension of 1 g of CAL-SBA-15 in 50 mL of toluene, 2 mL AzPTES were added, and the mixture was stirred for 16 h at 80 °C under nitrogen atmosphere. After the completion of reaction, the contents were cooled, filtered and washed with toluene until it became free from AzPTES. The sample was then dried at 80 °C for 8h in a vacuum oven and preserved under argon atmosphere for further use. Yield: ~1.2 g. This material will be referred as AZP-SBA-G.

Modification of AZP-SBA-C and AZP-SBA-G by Cu(I) catalyzed azide-alkyne cycloaddition reaction (CuAAC). For CuAAC, the azide functionalized SBA-15 (AZP-SBA-C or AZP-SBA-G) was incubated with 3 equivalents of the corresponding alkyne

(**1–4**, see Scheme 2) in a 1:1 water/t-butanol mixture containing $CuSO_4$ (1 equivalent) and sodium ascorbate (4 equivalent). In a typical click reaction, AZP-SBA-C (300 mg, 0.395 mmol of azide) was incubated with propargyl alcohol (70.07 μL, 1.185 mmol) in 10 mL of t-BuOH/water (1:1) containing sodium ascorbate (156.42 mg, 0.790 mmol) and copper sulfate (98.75 mg, 0.395 mmol). The mixture was stirred for 12 h and another 156.42 mg (2 equivalents) of sodium ascorbate was added and the reaction mixture was incubated for a further 12 h. After completion of reaction, the reaction mixture was centrifuged and the residue was first washed with water twice and then sequentially washed with 0.1 M N,N-diethyldithiocarbamate sodium in methanol (15 mL), methanol (15 mL), and acetone (15 mL) respectively. The last three washings were repeated thrice. Finally, the faint yellowish white powder obtained was dried at 80 °C in vacuum oven for 6–8 h. Yield: ~250 mg.

Note: Click reaction with α-D-propargyl mannopyranoside was carried out in water.

Labeling of SBA-C-4 with fluorescein labeled Concanavalin A. 10 mg of mannose labeled SBA-15 (SBA-C-**4**, see Table 1) or alcohol labeled SBA-15 (SBA-C-**1**, see Table 1) was incubated with fluorescently labeled Concanavalin-A (300μL, 1 mg/mL) in 20 mM Tris-HCl buffer (pH 7.4) containing 0.1 mM $MnCl_2$, 0.1 mM $CaCl_2$ and 0.15 M NaCl. After incubation for 30 min both samples were washed extensively (3 times) with the above mentioned buffer. The samples were dispersed in the buffer, and put under a microscope under both bright-field and epi-fluorescence modes (with a 470–490 nm bandpass filter).

Characterization

Powder X-ray diffraction of all the samples was carried out in a PANalytical X'pert Pro dual goniometer diffractometer. A proportional counter detector was used for low angle experiments and an X'celerator solid state detector was employed in the low angle experiments. The radiation used was Cu Kα (1.5418 Å) with a Ni filter and the data collection was carried out using a flat holder in Bragg-Brentano geometry (0.5 to 5°; 0.2° min^{-1}). Care was taken to avoid sample displacement effects. SEM images were obtained on Leica Stereoscan 440 microscope. HR-TEM images were taken on a FEI Technai F30 operating at 300 kV with FEG. The samples were prepared by dispersing a large number of solid particles in acetone by sonication, and dropping the resulting suspension on a copper grid of 400 mesh and allowed to dry in air. Nitrogen adsorption and desorption studies were carried out at 100 °C using a Micromeritics instrument.

Table 1 Yield of CuAAC reaction with different substrates

Mesoporous Material	Alkyne substrate	Product	CuAAC reaction yield (%)
AZP-SBA-C	Propargyl alcohol (**1**)	SBA-C-**1**	85
	Phenylacetylene (**3**)	SBA-C-**3**	63
	α-D(+)-propargyl mannopyranoside (**4**)	SBA-C-**4**	55
AZP-SBA-G	Propargyl alcohol (**1**)	SBA-G-**1**	90
	α-D(+)-propargyl mannopyranoside (**4**)	SBA-G-**4**	79

Samples were preheated at 100 °C for 12 hours in the vacuum line. Single point BET surface area was obtained from the nitrogen adsorption-desorption data at $P/P_0 \sim 0.249$. Pore size distributions were calculated using the BJH method. Semi-quantitative FT-IR spectra were recorded on a Perkin Elmer FT-IR spectrum GX instrument by making KBr pellets. Pellets were prepared by mixing 3 mg of sample with 97 mg of KBr. Yields for AAC reactions were calculated from corrected area under the curve characteristic for the azide stretch at ~2100 cm^{-1}. The average of three values was used for all calculations. Qualitative FT-IR spectra were recorded on a Perkin-Elmer spectrometer in the diffuse reflectance mode operating at a resolution of 4 cm^{-1}. Elemental analyses were carried out on a Thermo Finnigan FLASH EA 1112 series instrument.

Solid-state NMR. ^{29}Si and ^{13}C cross polarization magic angle spinning (CPMAS) NMR experiments were carried out on a Bruker AVANCE 300 wide bore spectrometer equipped with a superconducting magnet with a field of 7.1 Tesla. The operating frequencies for ^{13}C and ^{29}Si were 75.4MHz and 59.6MHz respectively. The samples were packed into a 4mm zirconia rotor and loaded into a 4mm BL MAS probe and spun about the magic angle (54.74) at 10kHz using a standard ramp-CP pulse sequence was used for both the experiments. The RF powers were 50kHz and 60kHz for the ^{29}Si and ^{13}C CPMAS experiments. The contact times were 6ms and 3ms for the ^{29}Si and the ^{13}C CPMAS experiments. All the chemical shifts were referenced to TMS. Typically 10000 to 25000 scans with a recycle delay of 3s were collected depending on the sensitivity of the sample.

Epi-fluorescence microscopy. Bright-field transmittance and epi-fluorescence microscopy was performed on samples that were drop-cast on glass cover slips. A 150mW Xe lamp and a 100mW halogen lamp attached to an inverted microscope (Nikon 2000U) were used as light sources to excite the samples for bright-field and epi-fluorescence modes, respectively, in order to show that the concentrations of the samples near the surface were approximately the same and the same areas were probed in both the imaging methods. For epi-fluorescence microscopy, proper excitation filters (470–490 nm bandpass filter, Chroma) were chosen to excite fluorescein. A Plan Apo 0.6 NA 40X air-objective was used to collect the fluorescence (500–580 nm emission filter, Chroma), which was subsequently imaged using a color digital camera (Nikon 4500) equipped with a 10× eyepiece and a home-built microscope adapter. For bright-field images, the exposure time was set at 30 ms, while the epi-fluorescence images were captured at lower excitation powers at 250 ms exposure to avoid photobleaching of samples. The images were processed using NIH ImageJ image analyses software and the raw data for both the sample and the control were adjusted to the same brightness and contrast levels to ensure that the stark contrast was clearly visible in the electronic format.

Results and discussion

Synthesis strategy of azide functionalized SBA-15

The azide functionalized SBA-15 was synthesized by both one-pot co-condensation and post-synthetic grafting methods as presented in Scheme 1. During the synthesis of AZP-SBA-C *via*

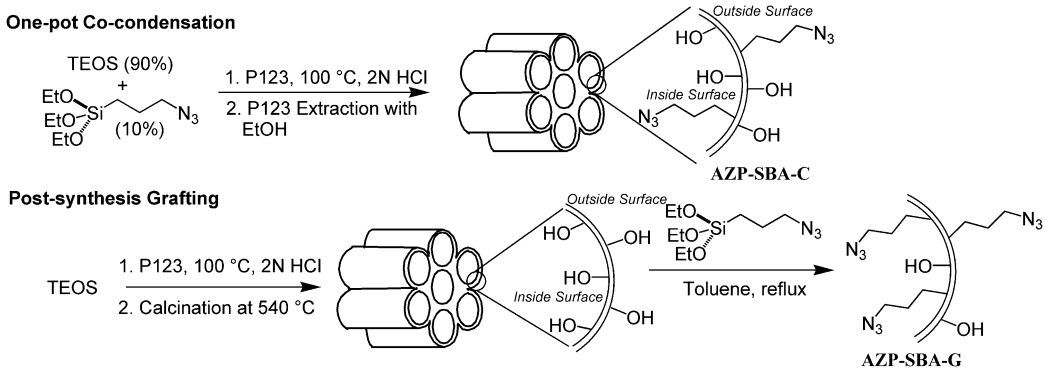

Scheme 1 Synthesis of azide functionalized SBA-15 materials.

one-pot co-condensation, the ratio of TEOS and AzPTES was kept as 9:1 since the usage of higher amounts of organosilica precursor may lead to functionalized materials with reduced long range order.[15] The organosilica precursor AzPTES was obtained by the displacement of the chloro group in 3-chloropropyltriethoxysilane with an azido group using sodium azide. In the post-synthetic grafting method, 1 g of calcined SBA-15 (CAL-SBA-15) was reacted with 8.1 mmol of AzPTES in toluene at 80 °C under an inert atmosphere to synthesize AZP-SBA-G. The amount of azidopropyl group that was incorporated into the SBA-15 framework was determined by elemental analysis. The concentration of azide was found to be 1.9 mmol/g for AZP-SBA-G while that for AZP-SBA-C was found to be 1.3 mmol/g. Therefore, during co-condensation, approximately 85% of AzPTES added was incorporated into the silica framework of AZP-SBA-C. The amount of azide incorporated in these materials was estimated to be doubled when HPLC grade silica beads[36] were used as the support matrix. The structure and morphology of AZP-SBA-C and AZP-SBA-G was established unambiguously using XRD, TEM, SEM, NMR and N_2 adsorption-desorption isotherms, as discussed below.

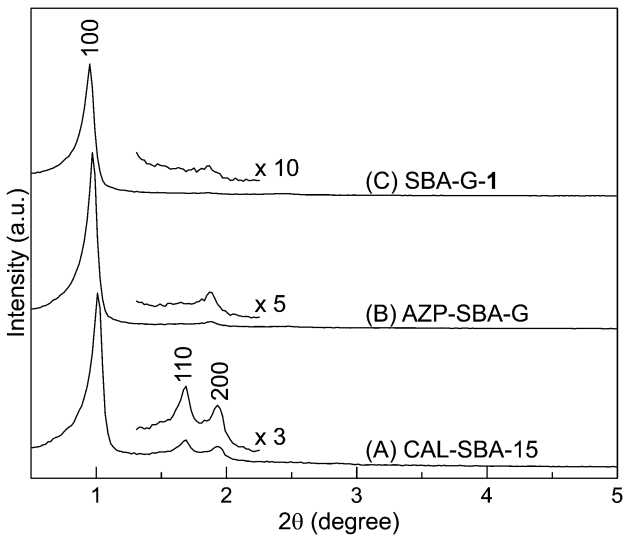

Fig. 1 Powder XRD patterns of different SBA-15 samples *via* post-synthesis grafting: [A] CAL-SBA-15; [B] AZP-SBA-G; [C] SBA-G-1.

Characterizations

The powder XRD patterns of grafted AZP-SBA-G and co-condensed AZP-SBA-C are shown in Fig. 1 and 2 respectively. All of the materials showed the characteristic high intensity 100 peak near the 2θ value of 1°. The other significant peaks corresponding to 110 and 200 diffractions were also observed indicating that well-ordered one-dimensional hexagonal mesoporous channels of SBA-15 were formed and remained intact under the functionalization environment. However, the higher order (110) and (200) diffractions become significantly less resolved for the azide-functionalized samples AZP-SBA-G (Fig. 1, curve B) and AZP-SBA-C (Fig. 2, curve A), showing that the long-range order decreases slightly upon incorporation of azidopropyl groups into the SBA-15 matrix. A similar phenomenon has been observed in aminopropyl-functionalized SBA-15 by Wang and co-workers.[15]

The SEM images displayed highly dispersed wormlike external morphology while the TEM micrographs showed the long parallel channel-structure with thick walls of the mesoporous materials AZP-SBA-G and AZP-SBA-C respectively (Fig. 3). The TEM and SEM pictures indicate that the mesoporosity was retained in both the azide grafted SBA-15 materials. Hence both

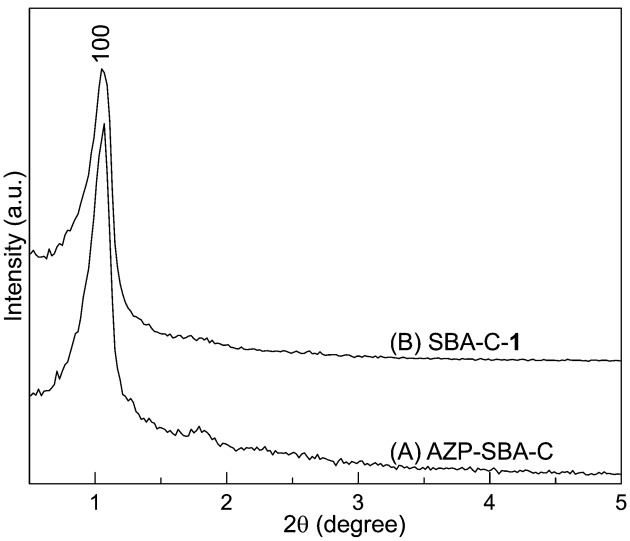

Fig. 2 Powder XRD patterns of different SBA-15 samples *via* co-condensation: [A] AZP-SBA-C; [B] SBA-C-1.

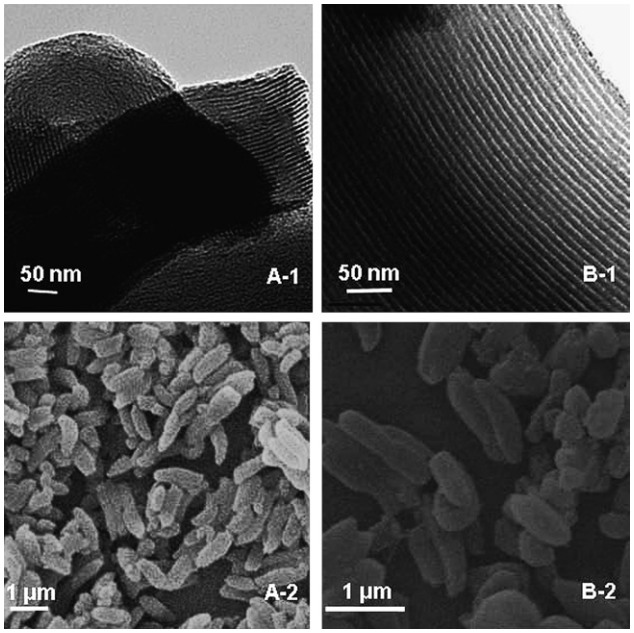

Fig. 3 SEM images and TEM micrographs of different azido-functionalized SBA-15 materials. A-1 and A-2 for AZP-SBA-G; B-1 and B-2 for AZP-SBA-C.

the grafting and co-condensation techniques did not interfere with the structural properties of SBA-15. N_2 adsorption-desorption isotherms of AZP-SBA-C exhibit the characteristic type IV isotherm with steep increase in adsorption at P/P_0 = 0.45–0.7 due to capillary condensation of the nitrogen in the mesopores.† The BJH pore-size distribution (PSD) analysis shows very narrow PSD values in the range 4–6 nm. The pore diameter, BET surface, micropore surface area and the wall thickness were determined to be 5 nm, 503 m^2/g, 92.3 m^2/g and 3.7 nm respectively.† These values are consistent with other organo-functionalized SBA-15 materials that have been reported before.[15–17,19]

The FT-IR spectra of the various functionalized SBA-15 materials are presented in Fig. 4. The spectra of both the azido-functionalized SBA-15 materials (AZP-SBA-C and AZP-SBA-G) display an absorbance at ~2100 cm^{-1} which is a characteristic stretching vibration of any organic azide (N_3). The absence of this peak in CAL-SBA-15 showed that the azidopropyl group has been successfully incorporated into both AZP-SBA-C and AZP-SBA-G sample. The samples showed absorbance peaks at 1220, 1070, 800 and 466 cm^{-1} respectively. These peaks are typical of Si–O–Si bands that are associated with the formation of the silica networks. Weak peaks associated with Si–OH groups in the 940–960 cm^{-1} range were also observed for the functionalized mesoporous materials. The strong peak around 1630 cm^{-1} might be attributed to the bending vibration of H_2O. Therefore, the FT-IR spectra indicate that the azido group was efficiently incorporated in the matrix of the mesoporous SBA-15 both by post-synthesis grafting and one-pot co-condensation techniques.

Fig. 5 represents the solid state ^{13}C CP-MAS NMR spectra of the functionalized SBA-15 materials. The spectrum of the as-synthesized azido-functionalized SBA-15 material synthesized using the co-condensation technique (as-synthesized AZP-SBA-C, Fig. 5a) displays signals for both the surfactant

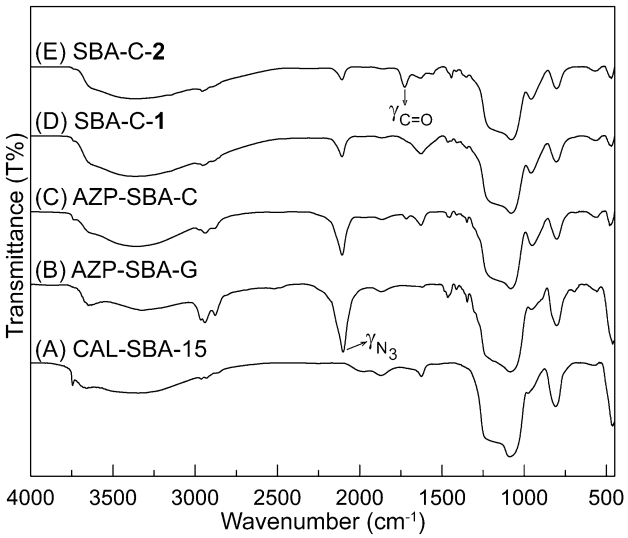

Fig. 4 Comparative FT-IR spectra of the different SBA-15 materials.

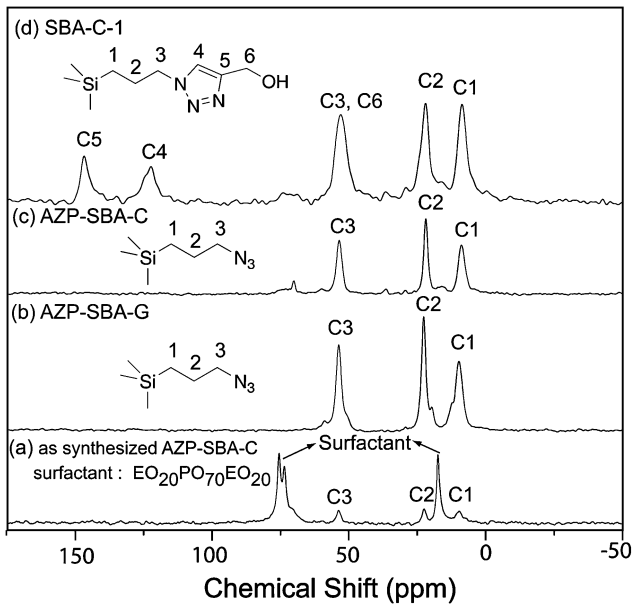

Fig. 5 ^{13}C CP MAS NMR spectra of the different functionalized SBA-15 materials.

$EO_{20}PO_{70}EO_{20}$ and azidopropyl group. The peaks at ~21 and 78 ppm correspond to the peaks for the surfactant while the three peaks C1 (8.68 ppm), C2 (22 ppm), C3 (53 ppm) represent the three C-atoms of the azido-propyl chain in the order as presented. The relative intensities of the C1, C2, C3 peaks appear to be less in comparison to the surfactant peaks because of the higher concentration of the latter in the as-synthesized matrix. After the as-synthesized AZP-SBA-C was extracted with ethanol to remove surfactant, the peaks characteristic of the surfactant disappeared, while the C1, C2, and C3 peaks of the azido-propyl group remained (Fig. 5b). The ^{13}C CP MAS NMR spectrum of AZP-SBA-G also showed three distinct peaks corresponding to the C1, C2. C3 carbon atoms (Fig. 5c). The ^{13}C CP-MAS NMR spectra of both AZP-SBA-C and AZP-SBA-G were similar

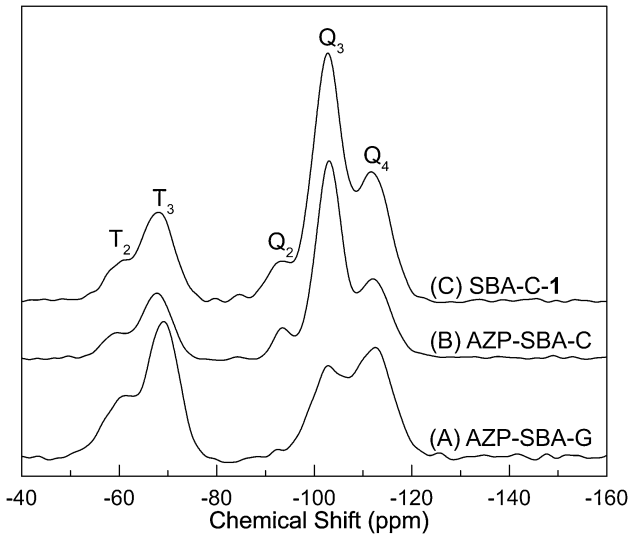

Fig. 6 ^{29}Si CP MAS NMR spectra of the different functionalized SBA-15 materials.

which indicated that the same material was produced by co-condensation and grafting.

The ^{29}Si CP MAS NMR spectra of the different azide-functionalized SBA-15 materials are presented in Fig. 6. All three spectra display prominent peaks at around −93, −102 and −112 ppm respectively. These may be assigned to the different types of Si sites namely Q^2 [$(SiO)_2Si(OH)_2$], Q^3 [$(SiO)_3Si(OH)$] and Q^4 [$(SiO)_4Si$] that are classified based on the total number of silanol groups (Si–OH) at the Si centre (*i.e.* 2, 1, 0 respectively). The ^{29}Si MAS spectra were obtained to evaluate the relative intensities of Q^3 and Q^4 for both AZP-SBA-C and AZP-SBA-G.† It was observed that in both the samples that the intensity of the Q^4 signal was found to be higher than the Q^3 signal. This is expected since SBA-15 is a thick-walled material in which much of the Si exists as $(SiO)_4Si$. Two other distinct peaks that are observed at −59.9 and −68 ppm may be attributed to the functionalized sites of the Si framework namely T^2 [$R(SiO)_2Si(OH)$] and T^3 [$R(SiO)_3Si$] respectively, where R is the azidopropyl group.

CuAAC of N_3-SBA-15 with various alkyne containing substrates

The azidopropyl labeled silicas AZP-SBA-C and AZP-SBA-G were subjected to Cu(I) catalyzed azide alkyne cycloaddition reaction (CuAAC) with various organic substrates (Scheme 2). Propargyl alcohol (**1**) was used as the substrate during the initial experiments to optimize the reaction conditions. The CuAAC reaction was attempted using $CuSO_4$/ascorbate in an equimolar mixture of t-BuOH and water. For example, treatment of AZP-SBA-C (25 mg) with **1** (0.1 mmol, 3-fold molar excess with respect to azide groups on azidopropyl grafted silica) using $CuSO_4$/ascorbate in 1:1 H_2O/t-BuOH for 24 h converted 85% of the available azide groups into the corresponding triazole product. Control reactions performed without the use of $CuSO_4$ showed no conversion of the azide. After the reaction, an extensive washing protocol was followed to remove the Cu(I), ascorbate and any unreacted **1**. One of the key steps in the washing was the use of dithiocarbamate to remove the Cu(I), as reported earlier.[40] Attempts to remove copper by using other chelating reagents like pH 8 Na_2EDTA led to the loss of a significant amount of the SBA-15 material indicating that a part of the silica had leached out during this process. Use of higher amounts of catalyst and longer reaction times did not improve the yield of the reaction. The extent of the reaction was estimated using IR spectroscopy, by monitoring the decrease in the integrated intensity of $\nu_{as}(N_3)$ at 2100 cm^{-1} (Fig. 4D, SBA-C-**1**). To get a semi-quantitative estimate of the conversion of the azide upon CuAAC, a calibration curve was made using quantitative amounts of AZP-SBA-C or AZP-SBA-G in KBr and plotting the integrated intensities of the azide IR peak at 2100 cm^{-1} to the concentration of the azidopropyl labeled silica in the KBr pellet.† We were, however, unable to observe the appearance of a 1,2,3-triazole stretch since it interfered with a strong peak at 1650 cm^{-1} from the bending vibration of water adsorbed to SBA-15. Since we were unable to observe the appearance of the triazole peak in the IR, we turned our attention to finding substrates that have a characteristic IR peak that does not interfere with the azide functionalized SBA-15 materials. For such substrates, their successful attachment would allow us to follow the reaction both by the appearance of their signature IR peak and with the disappearance of the azide stretch of the starting SBA-15 material. The methyl ester of 2-pentynoic acid (**2**) was thus chosen as the substrate for CuAAC since it had a characteristic carbonyl stretch at 1727 cm^{-1}, a region that displayed no peaks for the azide labeled SBA-15 materials. The successful attachment of **2** was confirmed from the IR spectra in which concomitant disappearance of $\nu_{as}(N_3)$ at 2100 cm^{-1} and the appearance of ν(C═O) at 1727 cm^{-1} was observed (Fig. 4E, SBA-C-**2**).

The dependence of the substrate concentration for the conversion of the available azide groups on AZP-SBA-C or AZP-SBA-G by CuAAC is shown in Fig. 7. Treatment of AZP-SBA-G (100 mg) with 1.5 equivalents of propargyl alcohol led to the formation of SBA-C-**1** in which 90% of all available azides were converted to the triazole (Table 1). Similar results were obtained with AZP-SBA-C although 3 equivalents of propargyl alcohol were needed to convert 85% of the available azides. The very high extent of the reaction leads us to conclude that in AZP-SBA-C, most azides are present in the surface of SBA-15. These data are in contrast to amino grafted SBA-15 material that was synthesized by co-condensation with aminopropyltriethoxysilane.[41] In this

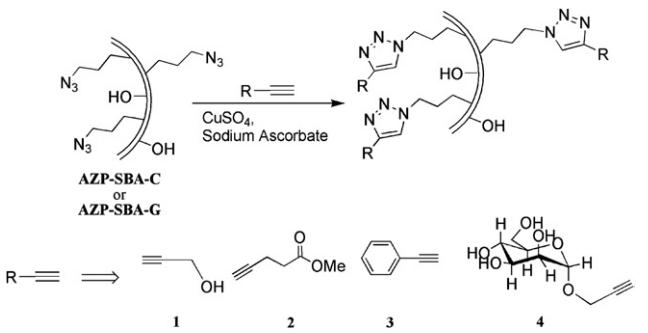

Scheme 2 CuAAC reaction of azide-functionalized SBA-15 with various substrates.

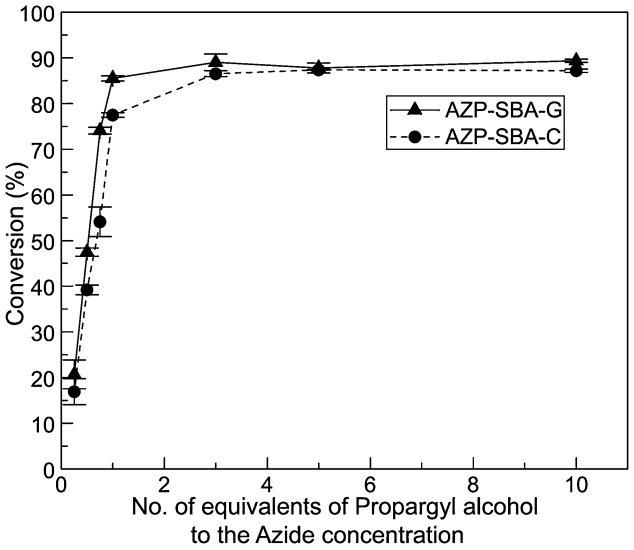

Fig. 7 Dependence of the percentage of azide converted in AZP-SBA-C or AZP-SBA-G on propargyl alcohol concentration. Reactions were performed with 100 mg of the respective azide functionalized SBA-15 material in 3 ml H_2O/t-BuOH (1:1) containing $CuSO_4$ (0.13 mmol) and sodium ascorbate (0.26 mmol).

material it was observed that only 25% of the available amino groups are on the surface. Since the azidopropyl group is more hydrophobic than the protonated aminopropyl group, it can act as a co-surfactant and be solubilized by the Pluronic micelles leading to its presence in the micelle-silica interface. The presence of the azides at this interface during synthesis is probably the reason for its high density at the surface of AZP-SBA-C. The presence of the azides mostly on the surface of AZP-SBA-C coupled with the very high efficiency of the CuAAC reaction makes AZP-SBA-C a very attractive material for attachment of alkyne containing functional molecules. It should also be noted that the percentage of available azide for click reaction is more in AZP-SBA-G than in AZP-SBA-C. This can be explained by the fact that during the direct synthesis of AZP-SBA-C by co-condensation, some of the azides may be trapped in the wall and therefore be unavailable for conjugation.

The product SBA-C-**1**, formed upon reaction of AZP-SBA-C and **1**, was further characterized by XRD, ^{13}C NMR and ^{29}Si NMR. The XRD showed one intense (100) peak diffraction in the proximity of $2\theta = 1°$, indicating well-ordered hexagonal arrays and showing that the mesoporosity of the material does not change after undergoing CuAAC reaction (Fig. 1C and 2B). The ^{13}C NMR shows extra peaks at 122 ppm and 146.7 ppm which correspond to the C4 and C5 atoms of the triazole as shown in Fig. 5d. The extra peak due to the C6 carbon is not observed as it is masked by the C3 peak from the linker. The ^{29}Si CP MAS spectrum of the SBA-C-1 material shows little or no change from the starting AZP-SBA-C indicating that the Si sites does not undergo any chemical change during the reaction and its work-up (Fig. 6C). This is expected since the T^1 and T^2 Si sites are from the azido-propyl modified silica and should not undergo any change during the course of the click reaction.

We then extended the CuAAC to other substrates to explore the efficiency of this reaction on azidopropyl functionalized SBA-15. The reaction was carried out with a five-fold excess of phenylacetylene (**3**), and α-D(+)-propargyl mannopyranoside (**4**) as substrates. The extent of the click reaction as observed using IR as described before is shown in Table 1. Both the substrates were successfully incorporated into the azido functionalized SBA-15 by CuAAC. The conversion of available azides was less for both phenylacetylene and α-D(+)-propargyl mannopyranoside than for propargyl alcohol. There may be several factors responsible for this observation. One of them is that propargyl alcohol, a much smaller molecule, is accessible to more azides during the click reaction.

The presence of mannose in the α-D(+)-propargyl mannopyranoside labeled SBA-15, SBA-C-**4**, was confirmed by probing its affinity for the protein Concanavalin-A (Con-A). The plant lectin Con-A exists as a tetramer in Tris-HCl buffer (pH 7.4) and binds up to four α-D(+)-mannopyranoside units in the presence of Na^+, Ca^{2+} and Mn^{2+} ions. Commercially available fluorescein labeled Con-A (300 μg) was incubated with both SBA-C-**4** and SBA-C-**1** (10 mg) in Tris-HCl buffer containing Na^+, Ca^{2+} and Mn^{2+} ions. After incubation for 30 min both the samples were extensively washed with Tris-HCl buffer containing Na^+, Ca^{2+} and Mn^{2+} ions. The samples were dispersed in the above mentioned buffer and were then put under a microscope under both bright-field and epi-fluorescence modes (with a 470–490 nm bandpass filter). The fluorescence observed from SBA-C-**4** incubated with Con-A is much more intense than that of the corresponding SBA-C-**1** that was incubated with Con-A (Fig. 8). The intense fluorescence is observed since the fluorescently labeled Con-A will bind to the mannose on the exterior surface of SBA-C-**4**. The material SBA-C-**1** was used as a control to eliminate the effect of triazole on the binding on Con-A. The diameter of tetrameric Con-A (each subunit is around 4.2 nm × 3.9 nm × 2 nm)[42] is larger than the pore size of SBA-C-**4** (5 nm) and this would probably attach to the mannose on the external surface of SBA-C-**4**, rather than inside the channels. The observance of intense fluorescence in Fig 8D indicates that mannose successfully conjugates to AZP-SBA-C to form SBA-C-**4** *via* CuAAC. The weak fluorescence observed in SBA-C-**1** is

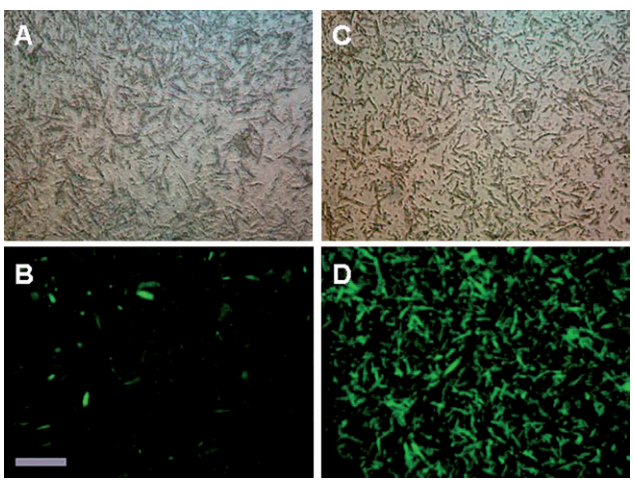

Fig. 8 A) SBA-C-**1** treated with fluorescent labeled Con-A in bright field mode. B) SBA-C-**1** treated with fluorescent labeled Con-A in epi-fluorescence mode. C) SBA-C-**4** treated with fluorescent labeled Con-A in bright field mode. D) SBA-C-**4** treated with fluorescent labeled Con-A in epi-fluorescence mode. The scale bar shown is equivalent to 10 microns.

probably due to the non-specific interaction between fluorescently labeled Con-A with the hydroxyl groups of silica or the 1,2,3-triazole functional group of SBA-C-**1**. This specificity of Con-A for mannose-labeled SBA-15 can be used in the development of sensors. Similar sensors have been developed for sensing ion transport in ion channels using the interaction of biotin-labeled MCM-41 with the protein avidin.[11]

Conclusion

The synthesis of azide labeled SBA-15 has been successfully achieved using both the one-pot co-condensation and post-synthetic grafting methods. The azide labeled SBA-15 materials retains their mesoporosity after synthesis and the incorporation of the organic functionality was confirmed by IR and solid state NMR. These materials undergo very efficient CuAAC with a variety of alkynes. When AZP-SBA-G was used, only 1.5 eq of alkyne was required to covert 90% of the available azides to triazole. Similar efficiency is very difficult to attain in aqueous solution by using amine and carboxylic labeled SBA-15, which are materials typically used to anchor various functional molecules. The azide labeled SBA-15 was further used as a platform to synthesize a silica-protein hybrid material composing of mannose labeled SBA-15 and Con-A. Such hybrid materials may be important in the development of biosensors. The ease of synthesis for the azide labeled SBA-15 material together with its ability to undergo very efficient chemoselective CuAAC in water would make it a very attractive platform for the development of covalently anchored catalysts, enzymes and sensors. Such efforts are under way in our laboratory.

Acknowledgements

BM, BRS and DP acknowledge CSIR, New Delhi, India for fellowships. SSG acknowledges Professor G. Ranga Rao, IIT-Madras, for help regarding BET analysis and Professor Arindam Chowdhury, IIT-Bombay, for help regarding fluorescence microscopy. SSG also acknowledges Dr CVV Satyanaryana, NCL for helpful discussions and NCL start-up grant and DST, New Delhi (Grant No: SR/S1/PC-56/2008) for funding.

References

1 B. G. Trewyn, I. I. Slowing, S. Giri, H.-T. Chen and V. S. Y. Lin, *Accounts of Chemical Research*, 2007, 846–853.
2 G. E. Fryxell, *Inorganic Chemistry Communications*, 2006, **9**, 1141–1150.
3 Y. Wan and D. Y. Zhao, *Chemical Review*, 2007, **107**, 2821–2860.
4 B. Kesanli and W. Lin, *Chem. Commun.*, 2004, 2284–2285.
5 C. Nozaki, C. G. Lugmair, A. T. Bell and T. D. Tilley, *Journal of the American Chemical Soceity*, 2002, **124**, 13194–13203.
6 T. J. Terry, G. Dubois, A. Murphy and T. D. P. Stack, *Angewandte Chemie International Edition*, 2007, **46**, 945–947.
7 H. Lakhiari, E. Legendre, D. Muller and J. Jozefonvicz, *Journal of Chromatography B: Biomedical Sciences and Applications*, 1995, **664**, 163–173.
8 J. E. Schiel, R. Mallik, S. Soman, K. S. Joseph and D. S. Hage, *Journal of Separation Science*, 2006, **29**, 719–737.
9 J. Li, T. Qi, L. Wang, C. Liu and Y. Zhang, *Materials Letters*, 2007, **61**, 3197–3200.
10 C. Y. Lai, B. G. Trewyn, D. M. Jeftinija, K. Jeftinija, S. Xu, S. Jeftinija and V. S. Y. Lin, *J. Am. Chem. Soc.*, 2003, **125**, 4451–4459.
11 K. Nozawa, C. Osono and M. Sugawara, *Sensors and Actuators, B: Chemical*, 2007, **126**, 632–640.
12 D. Zhao, Q. Huo, J. Feng, B. F. Chmelka and G. D. Stucky, *Journal of the American Chemical Soceity*, 1998, **120**, 6024–6036.
13 D. Zhao, J. Feng, Q. Huo, N. Melosh, G. H. Fredrickson, B. F. Chmelka and G. D. Stucky, *Science*, 1998, **279**, 548–552.
14 X. Wang, K. S. K. Lin, J. C. C. Chan and S. Cheng, *Chem. Commun.*, 2004, 2762–2763.
15 X. Wang, K. S. K. Lin, J. C. C. Chan and S. Cheng, *Journal of Physical Chemistry B*, 2005, **109**, 1763–1769.
16 Q. Wei, Z. Nie, Y. Hao, Z. Chen, J. Zou and W. Wang, *Materials Letters*, 2005, **59**, 3611–3615.
17 C.-m. Yang, B. Zibrowius and F. Schuth, *Chemistry of Materials*, 2003, 1772–1773.
18 R. Marschall, J. Rathousk and M. Wark, *Chemistry of Materials*, 2007, **19**, 6401–6407.
19 Q. Wei, H.-Q. Chen, Z.-R. Nie, Y.-L. Hao, Y.-L. Wang, Q.-Y. Li and J.-X. Zou, *Materials Letters*, 2007, **61**, 1469–1473.
20 A. Stein, B. J. Melde and R. C. Schroden, *Advanced Materials*, 2000, **12**, 1403–1419.
21 M. Hartmann, *Chemistry of Materials*, 2005, **17**, 4577–4593.
22 H. H. P. Yiu, P. A. Wright and N. P. Botting, *Journal of Molecular Catalysis B: Enzymatic*, 2001, **15**, 81–92.
23 Y. Zhu, S. Kaskel, J. Shi, T. Wage and K.-H. van Pee, *Chemistry of Materials*, 2007, **19**, 6408–6413.
24 Y. Zhu, W. Shen, X. Dong and J. Shi, *Journal of Materials Research*, 2005, **20**, 2682–2690.
25 J. Kim, J. W. Grate and P. Wang, *Chemical Engineering Science*, 2006, **61**, 1017–1026.
26 H. H. P. Yiu, P. A. Wright and N. P. Botting, *Microporous and Mesoporous Materials*, 2001, **44–45**, 763–768.
27 A. S. M. Chong and X. S. Zhao, *Catalysis Today*, 2004, **93–95**, 293–299.
28 J. He, X. Li, D. G. Evans, X. Duan and C. Li, *Journal of Molecular Catalysis B: Enzymatic*, 2000, **11**, 45–53.
29 P. Wang, S. Dai, S. D. Waezsada, A. Y. Tsao and B. H. Davison, *Biotechnology and Bioengineering*, 2001, **74**, 249–255.
30 I. S. Carrico, *Chem. Soc. Rev.*, 2008, **37**, 1423–1431.
31 V. V. Rostovtsev, L. G. Green, V. V. Fokin and K. B. Sharpless, *Angewandte Chemie International Edition*, 2002, **41**, 2596–2599.
32 V. D. Bock, H. Hiemstra and J. H. van Maarseveen, *European Journal of Organic Chemistry*, 2006, **2006**, 51–68.
33 A. J. Dirks, J. J. L. M. Cornelissen, F. L. Van Delft, J. C. M. Van Hest, R. J. M. Nolte, A. E. Rowan and F. P. J. T. Rutjes, *QSAR and Combinatorial Science*, 2007, **26**, 1200–1210.
34 L. Jean-François, *Angewandte Chemie International Edition*, 2007, **46**, 1018–1025.
35 D. A. Fleming, C. J. Thode and M. E. Williams, *Chemistry of Materials*, 2006, **18**, 2327–2334.
36 Z. Guo, A. Lei, X. Liang and Q. Xu, *Chem. Commun.*, 2006, 4512–4514.
37 K. M. Kacprzak, N. M. Maier and W. Lindner, *Tetrahedron Letters*, 2006, **47**, 8721–8726.
38 S. Ciampi, T. Bocking, K. A. Kilian, J. B. Harper and J. J. Gooding, *Langmuir*, 2008, **24**, 5888–5892.
39 Q. Wang, T. R. Chan, R. Hilgraf, V. V. Fokin, K. B. Sharpless and M. G. Finn, *Journal of the American Chemical Society*, 2003, **125**, 3192–3193.
40 T. J. Terry and T. D. P. Stack, *Journal of the American Chemical Soceity*, 2008, **130**, 4945–4953.
41 J. M. Rosenholm and M. Linden, *Chemistry of Materials*, 2007, **19**, 5023–5034.
42 G. M. Edelman, B. A. Cunningham, G. N. Reeke, J. W. Becker, M. J. Waxdal and J. L. Wang, *Proceedings of the National Academy of Sciences for the United States of America*, 1972, **69**, 2580–2584.

